

Driven Response of a Trapped Particle Beam

T. Satogata,⁽¹⁾ T. Chen,⁽²⁾ B. Cole,⁽³⁾ D. Finley,⁽¹⁾ A. Gerasimov,⁽¹⁾ G. Goderre,⁽¹⁾ M. Harrison,⁽⁴⁾
 R. Johnson,⁽¹⁾ I. Kourbanis,⁽¹⁾ C. Manz,⁽⁵⁾ N. Merminga,⁽⁵⁾ L. Michelotti,⁽¹⁾ S. Peggs,⁽¹⁾ F. Pilat,⁽³⁾
 S. Pruss,⁽¹⁾ C. Saltmarsh,⁽³⁾ S. Saritepe,⁽¹⁾ R. Talman,^{(2),(3)} C. G. Trahern,⁽³⁾ and G. Tsironis⁽⁶⁾

⁽¹⁾Fermi National Accelerator Laboratory, Batavia, Illinois 60510

⁽²⁾Newman Laboratory of Nuclear Studies, Cornell University, Ithaca, New York 14853

⁽³⁾SSC Laboratory, Dallas, Texas 75237

⁽⁴⁾Brookhaven National Laboratory, Upton, New York 11973

⁽⁵⁾Stanford Linear Accelerator Center, Stanford, California 94305

⁽⁶⁾Physics Department, University of North Texas, Denton, Texas 76203

(Received 20 December 1991)

The dynamics of a metastable beam of particles “injected” into artificially excited resonance islands in the Fermilab Tevatron is studied. Evolution of the captured beam distribution is measured by an externally detectable coherent signal. Dynamical partitions observed in the control space of amplitude and tune of a focusing modulation are consistent with an equivalent model of an ensemble of driven gravity pendula. The model’s single parameter, the island tune Q_I of small oscillations, is inferred as the central frequency of resonant detrapping under this weak drive.

PACS numbers: 41.75.Ak, 03.20.+i, 05.45.+b, 29.20.Dh

The formation of a “metastable state” of a proton beam circulating in an accelerator, in which the particles are trapped on a resonance island, has previously been demonstrated [1]. This Letter describes an experiment performed at the Fermilab Tevatron to study the response of that state to an external drive. The protons were under the influence of a single dominant nonlinear resonance, caused by the strong excitation of fourteen sextupoles in the otherwise nearly linear accelerator. The island location was forced to oscillate at a modulation tune Q_m , with an amplitude proportional to the modulation amplitude q . (“Tune” is defined to be a frequency as a fraction of the accelerator revolution frequency.) An active subject of interest in the accelerator community is the extent to which sources of such modulation are responsible for storage time limitations. For example, theory and simulation of the “beam-beam” interaction (which somewhat affects the luminosity limit of the Tevatron) only become quantitatively consistent with reality when *ad hoc* tune modulation is incorporated [2].

At the start of each observation shot, about 10^{10} protons circulating in a single needle-shaped bunch were kicked horizontally with a typical “betatron” amplitude of 3 mm. An appreciable fraction (typically one-fourth) were captured on a resonance island. The location and size of the island were adjusted by varying sextupole strengths and the “base tune” of small-amplitude particles. The beam was then allowed to circulate for some 10 s to allow transients to decay before data were taken. The phase space evolution of the center of charge was observed by using two beam position monitors, separated by approximately 90° in betatron phase, which recorded the centroid position and centroid slope on each turn for 64000 turns (1.4 s).

Figure 1 shows the simulated motion of a family of

(unmodulated) protons. One dot is plotted per accelerator turn in a “Poincaré plot” in (a, ϕ) phase space, where the horizontal displacement at a beam position monitor on turn t is $a \sin(\phi)$. A proton launched with a small amplitude advances smoothly around a circle, with ϕ increasing by slightly less than $4\pi/5$ rad per turn, so that the net motion after five turns is small. The corresponding displacement of a single proton at a stationary reference point varies like a pure sinusoid, $\sin(2\pi Q_0 t)$, on successive turns labeled by an integer index t , where the base tune Q_0 is just less than 0.4. Higher harmonics of the tune become more important in a Fourier expansion of the displacement as the amplitude is increased. At the same time, the tune Q increases from the base tune, according to

$$Q(a) = Q_0 + \frac{1}{2} U a^2, \quad (1)$$

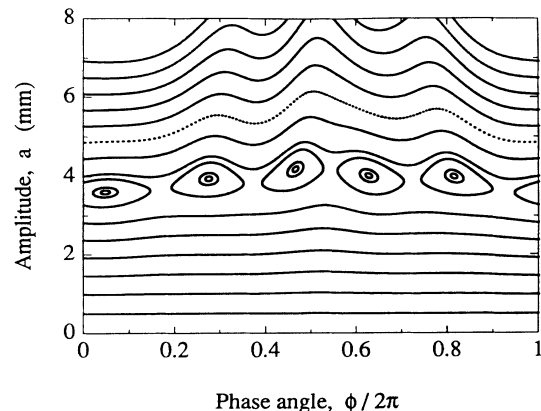


FIG. 1. Simulated phase space structure of the Tevatron, as distorted by fourteen strong sextupoles.

where the detuning coefficient U is given by

$$U = 0.000474 \text{ mm}^{-2}. \quad (2)$$

Earlier experiments, reported in these Letters and elsewhere, measured the variation of tune and of harmonic distortions versus amplitude under different sextupole conditions, successfully comparing experiment, simulation, and theory [1,3].

Resonance islands appear at intermediate amplitudes in Fig. 1. A proton launched inside one of the islands hops two islands per accelerator turn, returning to its original island after five turns. Since it never escapes the island (without tune modulation), a "resonant proton" only visits a localized range of phases. That is, it has a tune of exactly $\frac{2}{5}$, and is phase locked. If a significant number of protons are trapped inside a resonance island, they are visible in the beam position monitor data as a coherent "persistent signal." This is the fundamental diagnostic used in the experiment.

Motion on and close to the resonance is conveniently represented by the "five-turn" Hamiltonian

$$H_5 = 2\pi(Q_0 - \frac{2}{5})J + \frac{1}{2}UJ^2 - V_5J^{5/2}\cos(5\phi), \quad (3)$$

where the action $J \equiv a^2/2$, the coefficient U parametrizes detuning, and the coefficient V_5 represents the strength of the resonance. The canonical differential equations of motion are obtained by partial differentiation of H_5 :

$$\dot{\phi} = 2\pi(Q_0 - \frac{2}{5}) + UJ - \frac{5}{2}V_5J^{3/2}\cos(5\phi), \quad (4)$$

$$\dot{J} = -5V_5J^{5/2}\sin(5\phi). \quad (5)$$

The small net motion of the difference system is well approximated when this motion is integrated over a time step of $\Delta t = 5$ turns.

Tune modulation was turned on about 0.2 s after data taking began, by sinusoidally driving two weak quadrupoles, so that the base tune became

$$Q_0 = Q_{00} + q \cos(2\pi Q_m t). \quad (6)$$

The tune modulation strength and tune, q and Q_m , were linearly ramped for 1 s, and then turned off for the last 0.2 s of data taking. This deceptively simple perturbation is rich in the modifications it makes to the simple resonant behavior described above, and to the observable persistent signals. Realistic sources of tune modulation include power supply ripple and the coupling of longitudinal oscillations to transverse motion through chromaticity. Four distinct dynamical phases are predicted in the two-dimensional control parameter space of tune modulation strength and tune, (q, Q_m) , according to a general theoretical model that is summarized below [4-6]. Here we report the direct observation of the three regions that were experimentally accessible.

Figure 2 shows typical position data taken after most of the beam was kicked to overlap a resonance island, and after transients have been allowed to damp. The signal

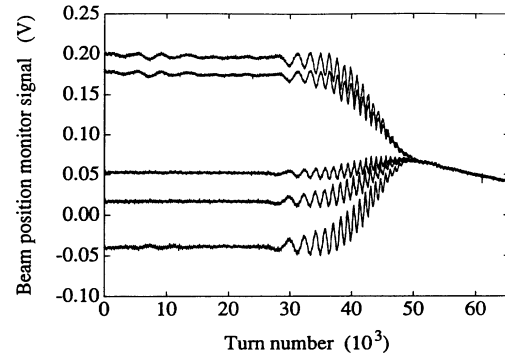


FIG. 2. Raw digitized signals of a beam position monitor, showing a persistent signal and its response to a chirp from $(q, Q_m) = (0, 0)$ to $(q, Q_m) = (0.0102, 0.0031)$. Vertical scale is in volts. Nonzero average initial value is due to a closed orbit offset.

from a beam position monitor was sampled and digitized once per accelerator turn as the single bunch passed by. For the first 27000 turns shown, the five discrete levels observed corresponded to the five unperturbed resonance islands. Protons outside the island had fractional tunes which were not exactly $\frac{2}{5}$, so they advanced faster or slower in phase than the captured portion of the beam, causing their transient contribution to the signal to decohere away in a few hundred turns. A more subtle transient effect concerned the distribution of protons inside the island. Protons close to the fixed point at the center of the island rotated at a characteristic "island tune" of Q_I , while protons further away rotated more slowly. This caused the distribution of trapped protons to evolve with a characteristic time of order $1/Q_I$ turns, until an equilibrium distribution was reached that was quite evenly spread over the island, since the initial beam size was somewhat larger than the island size. Tune modulation was turned on at 9000 turns, and became clearly visible as an amplitude modulation of the islands at about 28000 turns. The persistent signal started dropping dramatically at about 32000 turns, eventually driving all of the trapped beam out of the resonance island.

The tune modulation trajectory that caused this response is drawn as the dashed line labeled "A" in Fig. 3, showing that the signal was lost when the boundary between "amplitude modulation" and "chaos" was crossed. Figure 3 also summarizes results from a trajectory labeled "B" that had a very weak constant tune modulation strength of $q = 0.000204$, smaller or comparable to realistic operational values. The circles in Fig. 3 show that the same boundary consistently fits "strong" and "weak" trajectories A and B, and other intermediate data sets that were taken, but which are not detailed here. Figure 3 also shows boundaries between the four theoretically predicted regions. The island tune $Q_I = 0.0063$ was the only free parameter used to adjust the location of these boundaries, and to achieve the remarkably detailed agreement

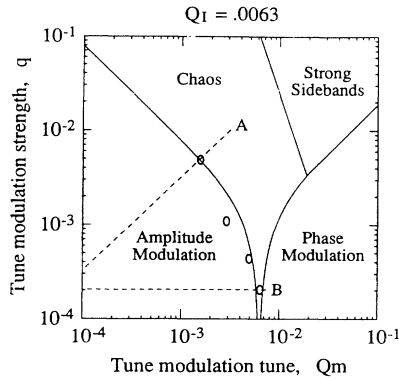


FIG. 3. Structure of the tune modulation parameter space (q, Q_m). A and B correspond to the scans shown in Figs. 2 and 4. Labeling of the four distinct “dynamical phases” is discussed in the text.

between experimental data and simulation data shown in Fig. 4 for the weak trajectory B .

Two different symbols represent experimental measurements in Fig. 4. Points with circles correspond to a single data shot, when Q_m was linearly chirped in 1 s from a start value of 0.0 to a maximum accessible end value of 0.00733, equivalent to 350 Hz. Points with diagonal crosses correspond to a series of seven data shots, in which the modulation tune was chirped in contiguous scans of width 0.00105, or 50 Hz. Three dynamical regions were reached in these scans—amplitude modulation, chaos, and phase modulation. Because the chaotic region was visited only briefly, a trapped beam was able to punch through into the stable phase modulation region, where the modulation tune was above the island tune. Access to this region was only just allowed by the experimental apparatus—modulated excitation of the quadrupoles was limited by their inductance. The persistent signal versus time was derived in a series of Fourier transforms of a raw beam position monitor signal at a tune of exactly $\frac{2}{5}$, with a sample time given by the horizontal spacing between data points. The vertical location of a data point is determined by the difference between neighboring persistent signal samples, normalized to give a decay rate measured in inverse turns. Vertical error bars represent the expected statistical significance of the decay rate, based on a knowledge of the signal-to-noise ratio in the Fourier spectra.

The solid line in Fig. 4 represents simulation results obtained by tracking an island evenly populated with protons under the influence of identical experimental conditions, and applying exactly the same data reductions. Details of the simulation technique, which was especially fast and simple, are available elsewhere [7]. Both the experiment and the simulation show evidence of structure at modulation tunes well below the island tune. It may be speculated that this is due to parametric modulation of the resonance strength, leading to Mathieu resonances at

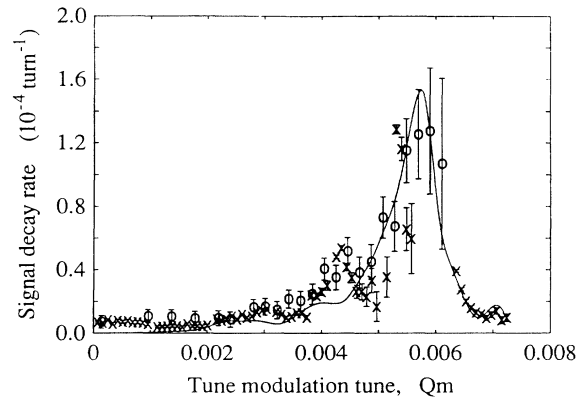


FIG. 4. Persistent signal decay rate as a function of tune modulation frequency Q_m in a scan where the tune modulation amplitude is held constant at $q = 2.04 \times 10^{-4}$. Symbols refer to experimental data, with circles representing data from a 350-Hz scan and crosses representing data from several contiguous 50-Hz scans. The line is a cubic spline fit through simulation data, with $Q_I = 0.0063$, for a single 350-Hz scan.

a family of modulation tunes given by $Q_m = 2Q_I/n$, for integer n [7]. However, the simplest way to generate parametric modulation, through the variation of the optical parameters at the sextupoles due to quadrupole perturbations, was explicitly absent in the simulation. Mathieu resonances are generated in other more indirect ways, and are visible in detailed single particle simulations that are not commented upon further here.

We now turn to a summary theoretical description of the experiment. Using the notation of Eqs. (1)–(6), the island tune Q_I is given by

$$Q_I = (5/2\pi)(UV_5 J_R^{5/2})^{1/2}, \tag{7}$$

where the “resonant action” J_R is the action at the fixed points of the mapping. Tune modulation is slow and weak in the lower left-hand corner of Fig. 3, so that the base tune Q_0 changes adiabatically. The island amplitudes change slowly as Q_0 changes slowly, but their phases are almost constant, justifying the amplitude modulation label. As the tune modulation strength q increases at constant modulation time Q_m , the stable area of the islands shrinks, analogous to the shrinkage of radio-frequency buckets as the ramp rate of an accelerator is increased. Eventually there is no stable area at all, and adiabatic trapping ceases to occur. The condition for this to happen (with fifth-order islands) is

$$qQ_m < Q_I^2/5. \tag{8}$$

The derivation of this relationship is rigorous in the slow limit, $Q_m \ll Q_I$, when a canonical transformation may be applied to the Hamiltonian [4].

Tune modulation is rapid but weak in the bottom right-hand corner of Fig. 3, causing the island fixed points to oscillate in phase, but not in amplitude. Addi-

tional chains of “modulation sideband” islands appear when the modulation strength q is large enough, at tunes around the fundamental labeled by the integer k , where

$$Q_k = \frac{2}{5} + k(Q_m/5). \quad (9)$$

Phase averaging techniques that are rigorous in the fast limit show that the k th sideband is negligibly small unless the modulation strength q is larger than its tune distance from the fundamental

$$q > |k|(Q_m/5). \quad (10)$$

This condition, with $k=1$, is the boundary between phase modulation and “strong sidebands” in Fig. 3. When sideband islands are present, the possibility of their phase space overlap must be considered, since the Chirikov overlap criterion states (loosely speaking) that this results in chaos [8]. Sidebands overlap and chaos ensues when

$$Q_m^{3/4} q^{1/4} < [4/(5\pi)^{1/4}] Q_I. \quad (11)$$

This line is drawn in Fig. 3 as the boundary between strong sidebands and chaos.

Finally, a small-angle analysis [6] shows that the two boundaries given by Eqs. (8) and (10) are plausibly and gracefully joined in the vicinity of the “resonance” $Q_m \approx Q_I$, where the modulation is neither fast nor slow, by the condition

$$qQ_m = |Q_I^2 - Q_m^2|/5. \quad (12)$$

It is not surprising that the most sensitive behavior occurs when the drive tune is near the free oscillation (island) tune. What is surprising is the simplicity and generality of the boundaries represented by Eqs. (8), (10), (11), and (12), when they are expressed in the “tune domain.” The experimental data presented above confirm the existence and location of these boundaries, insofar that the relevant parts of tune modulation parameter space were experi-

mentally available.

Realistic sources of tune modulation in an accelerator include power supply ripple and the coupling of longitudinal oscillations to transverse motion through chromaticity. The requirements made on these quantities are often severe—for example, if trajectory B in Fig. 3 is regarded as an upper limit. In that case, and if the Tevatron quadrupoles were on a separate bus from the dipoles (they are not), then a relative power supply ripple of only 1 part in 10^5 would be tolerated. Similarly, trajectory B corresponds to a net chromaticity of only 1.0 for a particle with an off-momentum amplitude of $\delta p/p_{\max} = 2 \times 10^{-4}$.

We would like to thank the Fermilab operations staff for their assistance and cooperation, and acknowledge the work of Keng Low, Matthew Kane, Michael Allen, Vern Paxson, Soam Acharya, and Kevin Cahill for their help in configuring the data acquisition system. We also thank George Bourianoff for helpful discussions.

- [1] A. Chao *et al.*, Phys. Rev. Lett. **61**, 2752 (1988).
- [2] S. Peggs and R. Talman, Annu. Rev. Nucl. Part. Sci. **36**, 287 (1986).
- [3] N. Merminga, Ph.D. thesis, University of Michigan, 1989 (unpublished).
- [4] S. Peggs, in *Proceedings of the Second ICFA Beam Dynamics Workshop*, edited by J. Hagel and E. Keil (CERN Report No. 88-04, Geneva, Switzerland, 1988), pp. 131–144.
- [5] T. Chen, S. Peggs, and G. Tsironis, in *Proceedings of the Second European Particle Accelerator Conference* (Editions Frontières, Gif-sur-Yvette, France, 1990), Vol. 2, pp. 1753–1755.
- [6] T. Chen, Superconducting Super Collider Laboratory Report No. 323, 1990 (unpublished).
- [7] T. Satogata and S. Peggs, in *Proceedings of the IEEE Particle Accelerator Conference*, San Francisco, 5–12 May 1991 (to be published).
- [8] B. Chirikov, Phys. Rep. **52**, 263 (1979).